

Direct Force Measurement of Silicone- and Hydrocarbon-Based ABA Triblock Surfactants in Alcoholic Media by Atomic Force Microscopy

Anfeng Wang, Liping Jiang,¹ Guangzhao Mao,² and Yihan Liu*

Department of Chemical Engineering and Materials Science, Wayne State University, Detroit, Michigan 48202; and *Dow Corning Corporation, Midland, Michigan 48686

Received September 19, 2001; accepted May 24, 2002

The surface force profiles between an atomic force microscopy (AFM) tip and a self-assembled monolayer of *n*-octadecyltrichlorosilane on oxidized silicon were measured in an ABA triblock series of silicone and Pluronic surfactant solutions. Changes in steric force barrier thickness and height were examined as a function of hydrophobic and hydrophilic block size and ethanol to water ratio in mixed solvents. In water, all the surface force profiles exhibited repulsive forces except for the Pluronic surfactants with short polyoxyethylene blocks. The steric barrier thickness increased with increasing hydrophilic block size, with an estimated force decay length proportional to (number of oxyethylene units)^{0.62}. However, the same data yielded no clear correlation between the hydrophobic chain block size and the steric barrier. The silicone surfactants provided steric repulsion up to 80% ethanol in solution, while the Pluronic surfactants lost their surface activity at approximately 40% ethanol in solution. The difference between the Pluronic surfactants and the silicone surfactants is attributed to the polysiloxane block being hydrophobic as well as oleophobic. In addition, the solubility and surface activity of silicone surfactants in alcoholic media are tunable by the ratio of oxyethylene to oxypropylene units. © 2002 Elsevier Science (USA)

Key Words: surface forces; steric repulsion; ABA triblock copolymers; silicone surfactant; Pluronic surfactant; polymer adsorption; colloidal stabilization; atomic force microscopy.

INTRODUCTION

Block copolymeric surfactants are widely used as detergents, emulsifiers, dispersing agents, and lubricants. The current understanding of the aggregation and adsorption of block copolymers (1–3) is made possible at least partially by the availability of many block copolymer series with well-defined composition and chain structure. Our own research into commercial block copolymeric surfactant series was prompted by the development of new surfactant series and surface characterization techniques. The surfactant series reported here belongs to the family of sil-

icone polyether (SPE) surfactants. The SPE surfactants exhibit several unique properties (4): (1) they can lower the air/water interfacial tension to about 20 mN/m; (2) the siloxane chain remains flexible and in the liquid state up to high molecular weight; (3) they are surface active in both aqueous and nonaqueous media; and (4) they are suitable for cosmetic applications because they cause little skin irritation. The base of the SPE surfactants is polydimethylsiloxane (PDMS). PDMS with sufficient molecular weight, e.g., about 1000, is well known for its hydrophobicity as well as oleophobicity. In particular, the oleophobicity distinguishes the silicone-based surfactants from their hydrocarbon counterparts. The molecular structure of SPEs is either comb-like, with the polyoxyalkylene chain side-grafted to a PDMS backbone, or linear diblock (AB) and triblock (ABA) types, with A representing the polyoxyalkylene hydrophile and B the PDMS hydrophobe. SPEs incorporating copolymers of polyoxyethylene (PEO) and polyoxypropylene (PPO) are widely used in polyurethane foam manufacture and personal care products. The incorporation of water-insoluble PPO should alter the aggregation behavior of SPEs in solution and at surfaces. However, neither their bulk nor surface aggregation behavior has been reported. This paper focuses on the adsorption behavior of the triblock type of SPEs, some with PEO/PPO copolymer hydrophiles, while the behavior of the comb type SPEs has been reported in a separate paper (5).

It is helpful to compare the aggregation behavior of silicone-based surfactants with the better known hydrocarbon-based surfactants, such as the Pluronic surfactants. The Pluronic surfactants, manufactured by BASF, are ABA triblock copolymers consisting of PEO as the A block and PPO as the B block. The Pluronic surfactants have been well characterized both in solution (6–8) and to a lesser extent at surfaces (6, 9–11). On the other hand, studies of the SPE surfactants are much more limited. To the best of our knowledge, the only published results are those that addressed the binary phase behavior of triblock SPE surfactants with oxyethylene homopolymer as the A block (12, 13). The Pluronic and SPE surfactants containing PEO homopolymers were found to follow the usual phase sequence of the low-molecular-weight ethoxylated fatty alcohols, progressing from the lamellar phase to the inverse hexagonal phase upon increasing temperature or decreasing the hydrophilic

¹ Current address: Paint and Coating Research Institute, Lanzhou, Gansu 730020, P. R. China.

² To whom correspondence should be addressed at Department of Chemical Engineering and Materials Science, Wayne State University, 5050 Anthony Wayne Drive, Detroit, MI 48202. E-mail: gzmao@che.eng.wayne.edu.

head group size. Pluronic surfactants have been reported to adsorb on a hydrophobic surface with the more hydrophobic PPO block anchoring as trains and loops and the PEO block extending into the solution as tails and loops. The hydrodynamic thickness of the adsorbed layer was found to increase with increasing PEO molecular weight. The thickness measured lies in between the length of a fully extended PEO chain and the radius of a random coil. The influence of PPO is less clear. The other extensively studied triblock surfactant series are the polyoxyethylene–polytetrahydrofuran–polyoxyethylene block copolymers (14, 15). The steric force barrier height was found to be equal to the surface pressure needed to expel the copolymers from the confinement gap. For the same B block, the repulsive barrier was found to increase with the A block size when measured on a hydrophobic surface. In another study of the adsorption of polyoxyethylene–polyoxybutylene diblock copolymer on hydrophobic silica and mica (16), the adsorbed configuration was described as a parabolic brush (3), in that the film thickness scales with $(\text{chain length} \times \text{chain density})^{1/3}$. A longer than expected range of repulsion was attributed to the polydispersity of the sample.

In addition to the effect of chain chemical composition, we are also interested in the effect of solvent on the adsorption behavior of SPEs. It was recently disclosed that oil-in-water emulsions made by certain SPEs are stable against alcohols and other organic solvents (17, 18). This is rather atypical since the addition of short-chained alcohols (with fewer than four carbon atoms) usually results in the decrease of the aggregation number and even the disappearance of micelles in solution, with a simultaneous loss in surface aggregation (19). This unusual attribute makes this class of SPE surfactants potentially very useful since alcohols are common cosolvents or additives in many emulsion and dispersion formulations. In order to explore this new phenomenon and to gain fundamental insights into the optimization of emulsions and dispersions, we carried out surface force measurements on both silicone-based and hydrocarbon-based surfactants in alcoholic media using atomic force microscopy (AFM). AFM (20) is a complementary force-measuring device to the traditional surface forces apparatus (SFA) (21). The primary difference between AFM and SFA force measurements is the radius of curvature of the interacting area prior to contact, around 10,000 μm for SFA, 5 μm for AFM with a colloidal tip, and 0.02 μm for AFM with a commercial silicon nitride tip. Therefore, AFM force curves tend to be shallower in the region of high compression than those from SFA, more sensitive to solvent quality and film inhomogeneity. Force curves obtained with silicon nitride tips were used to characterize surfactant films formed at the liquid/solid interface (22, 23). The AFM force measurement results of comb type SPE surfactants with varying hydrophilic structures have been reported earlier (5). The force measurement results compared consistently with those from emulsion-stability and interfacial-tension measurements. Here, we report the force measurement results on the adsorption behavior of ABA type SPE and Pluronic surfactants

at the solid/liquid interface in a mixed solvent of water and ethanol. The oxidized silicon covered by a self-assembled monolayer (SAM) of *n*-octadecyltrichlorosilane (OTS) was used as a model hydrophobic substrate in our study. The anchoring portion of the SPE surfactant is the polysiloxane block (B block) and the nonanchoring portion is the EO block or the EO/PO copolymer block (A block).

MATERIALS AND METHODS

Materials. One-sided polished silicon (111) wafers (test grade, N type, with resistivity 1 to 2 ohm-cm) were purchased from Wafer World. OTS was purchased from United Chemical Technologies and vacuum distilled before using. USP grade 190-proof and 200-proof ethanol was purchased from Pharmco Products and AAPER Alcohol and Chemical respectively. Carbon tetrachloride (>99.9%, HPLC grade) and *n*-hexadecane (>99%) were purchased from Aldrich. Chloroform (99.9%) was purchased from Fisher Scientific. Deionized water with a resistivity of 18 M Ω -cm was obtained from Barnstead Nanopure Systems.

The nominal structures of Pluronic and silicone surfactants are listed in Tables 1 and 2, respectively. All the polymeric surfactants were used as received. Pluronic surfactants were given by BASF. We selected surfactants whose cloud points are above room temperature and whose molecular weight range is similar to that of silicone surfactants. The average numbers of EO and PO units in each block are represented by *m* and *n*, respectively. The concentration of all Pluronic surfactants studied was fixed at 0.5% w/w, generally higher than the onset concentration of the pseudo-plateau in the adsorption isotherm on a hydrophobic surface ($\sim 0.01\%$ w/w on polystyrene latex), but lower than the critical micelle concentration (CMC ~ 3 to 11% w/w). This concentration was chosen in order to maximize the contribution

TABLE 1
Molecular Structure and Properties of Pluronic Surfactants Provided by BASF

Pluronic surfactant	Molecular weight	<i>m</i>	<i>n</i>	Polydispersity index ^a	HLB ^b
L62	2500	5.6	34.2	1.25	1–7
L64	2900	13.1	29.8	1.2	12–18
P65	3400	19.2	29.2		12–18
F68	8400	76.2	28.9	1.1	>24
P84	4200	19.0	43.3		12–18
P85	4600	26.0	39.5	1.06	85
F87	7700	61.1	39.7	1.60	>24
F88	11400	103.5	39.2	2.12	>24
P104	5900	26.7	60.8		12–18
P105	6500	36.8	55.9		12–18
P108	14600	132.6	50.3	2.24	>24

Note. The symbols *m* and *n* are the numbers of EO and PO units in A and B blocks, respectively.

^a Data were taken from Reference 9.

^b HLB is the hydrophilic–lipophilic balance.

TABLE 2
Molecular Structure of SPE Surfactants

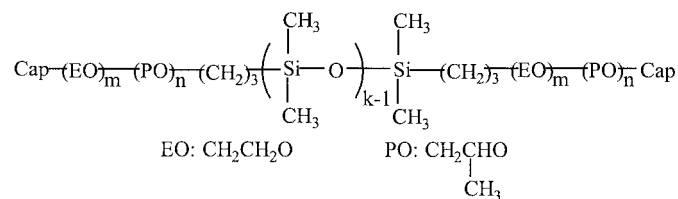
Abbreviation	<i>k</i>	<i>m</i>	<i>n</i>	Cap	M.W.	HLB ^a	CER ^b	HLB _{CER} ^b
E ₇ D ₁₅ E ₇	15	7	0	OH	1,828	6.74		
E ₁₂ D ₁₅ E ₁₂	15	12	0	OH	2,268	9.31		
E ₁₈ P ₁₈ D ₅₂ E ₁₈ P ₁₈	52	18	18	OH	7,622	4.16	0.69	11.3
E ₁₈ P ₁₈ D ₆₀ E ₁₈ P ₁₈	60	18	18	OH	8,214	3.86	0.79	10.7
E ₁₈ P ₁₈ D ₇₇ E ₁₈ P ₁₈	77	18	18	OAc	9,556	3.32	0.99	9.65

^a HLB values were calculated by the molecular weight percentage of the ethylene oxide portion divided by 5.

^b CER and HLB_{CER} values were calculated by a method developed by Beerbower and Hill (26, 27).

from surfactant aggregates at surface and in the meantime minimize the interference from aggregates in solution during the force measurement. The SPE surfactants were synthesized by Michael R. LaFore of the Dow Corning Corporation (24). The general chemical structure of the SPE surfactants is illustrated in Scheme 1. We adopted an abbreviation E_{*m*}P_{*n*}D_{*k*}E_{*m*}P_{*n*} for the SPE surfactants, where E, P, and D denote the oxyethylene, oxypropylene, and siloxane units, respectively, and *m*, *n*, and *k* denote the average degree of polymerization of the respective units. Cap denotes the type of capping group. The hydrophilic-lipophile balance (HLB) number is used as a practical numerical rating scheme for emulsion formulations (25). However as pointed out in an earlier paper (5), it is not suitable for silicone surfactants or for nonaqueous emulsions. Therefore we also provide the cohesive energy ratio (CER) developed by Beerbower and Hill (26, 27). CER is based on the molecular structure and solubility parameters and is a measure of the solubility “balance” of the emulsifier between the two liquid phases. The CER number was found to work better in the case of silicone surfactants. The concentration of all SPE surfactants studied here was fixed at 0.2% w/w, above the surfactant CMCs. The ethanol to water ratio was varied gradually. All the solutions were used within 1 week of preparation. The solution was filtered (0.45- μ m pore size, Millipore) prior to injection into the AFM liquid cell. The pH of the solution was measured between 3.67 and 8.09 by a Cole-Parmer pH benchtop meter (Niles).

Substrate surface treatment. The silicon wafer was cut to around 1 \times 1 cm² pieces, and the pieces were rinsed with water



SCHEME 1. General chemical structure of the ABA triblock SPE surfactants investigated. When both EO and PO were present in the polyether chain, they were randomly copolymerized.

and acetone, followed by the RCA clean procedures used in integrated circuit manufacturing (28). The treated substrate displayed a near zero static contact angle with water (NRL Contact Angle Goniometer, Model 100, Rame-Hart). A full monolayer of OTS was deposited from the solution phase onto the substrate (29). The water contact angle was measured to be $107 \pm 2^\circ$ on the substrate coated with the OTS monolayer.

Gibbs adsorption isotherms. While the phase diagram of these triblock SPE surfactants has never been studied, their CMC values were determined here by the Gibbs isotherm plot of surface tension versus logarithmic concentration. The air/solution interfacial tension was determined by the Wilhelmy plate method using a dynamic contact angle analyzer (DCA-312, Model 21200-02, Cahn). The solutions were let stand for about 2 h before measurement. Table 3 lists the apparent values of CMC, area per molecule, and surface tension at CMC of the five ABA siloxane surfactants used in this study. The CMCs decreased with decreasing hydrophilic chain length or increasing hydrophobic chain length as expected, with the exception of E₁₈P₁₈D₇₇E₁₈P₁₈, which exhibited a larger than expected CMC value. The CMC and area per molecule of the three larger molecules with propylene in the polyether chains are larger than the values of the two smaller molecules. The surface tension of the surfactants is around 32 mN/m, except for E₇D₁₅E₇, which has a surface tension around 25 mN/m.

Emulsion preparation and stability measurement. A typical recipe for the preparation of the oil-in-water emulsion is described as the following: (1) Part A was mixed in a container at 80°C. It contained 12 g of stearic acid (Hystrene 4516, Witco), 12 g of glyceryl stearate and PEG-100 stearate (Arlacel 165, ICI), and 30 g of mineral oil light; (2) Part B was mixed in another container at 60°C. It contained 406.6 g of water and 7.4 g of triethanolamine (85% active in water); (3) Part A was poured into Part B, and the mixture was agitated with a mixer at 400 rpm at 60°C for 1 h and then cooled to room temperature. This is called the thick phase; (4) Part C was made in a separate container. It contained 120 g of water and 12 g of an ABA SPE surfactant or the Pluronic surfactant P85; (5) the mixture made in step (3) was poured into Part C, and the final emulsion was agitated with a mixer at 350 rpm for half an hour. The above procedures were repeated for each of the ABA type surfactants.

TABLE 3
CMC, Area per Molecule, and Surface Tension at CMC Values Determined from Gibbs Plots

Surfactant	CMC (% w/w)	Area per molecule (nm ²)	Surface tension at CMC (mN/m)
E ₇ D ₁₅ E ₇	0.0140	0.311	25.6
E ₁₂ D ₁₅ E ₁₂	0.0152	0.477	31.8
E ₁₈ P ₁₈ D ₅₂ E ₁₈ P ₁₈	0.0237	0.684	32.4
E ₁₈ P ₁₈ D ₆₀ E ₁₈ P ₁₈	0.0188	0.513	31.9
E ₁₈ P ₁₈ D ₇₇ E ₁₈ P ₁₈	0.0238	0.580	32.2

TABLE 4

Comparison of Emulsion Stability Provided by ABA Triblock SPE Surfactants and the Pluronic Surfactant P85

Surfactant	30% Ethanol	90% Ethanol
E ₇ D ₁₅ E ₇	31.5 h (R)	13 min (P)
E ₁₂ D ₁₅ E ₁₂	22.0 h (R)	10 h (P)
E ₁₈ P ₁₈ D ₅₂ E ₁₈ P ₁₈	27.0 h (R)	<1 min (P)
E ₁₈ P ₁₈ D ₆₀ E ₁₈ P ₁₈	26.8 h (R)	<1 min (P)
E ₁₈ P ₁₈ D ₇₇ E ₁₈ P ₁₈	9 days (R)	<1 min (P)
P85	6 days (R)	<1 min (I)

Note. R stands for reversible phase separation (i.e., the emulsion was flocculated instead of coalesced after the indicated amount of time and was redispersed on shaking). P stands for partially reversible phase separation. I stands for irreversible phase separation.

An emulsion stability test was conducted by slowly adding an ethanol and water mixture to the emulsion while stirring. The final mixture was let stand for observation of phase separation.

The results are summarized in Table 4. All the surfactants showed ability to emulsify oil in water in low to intermediate ethanol levels, with the higher molecular weight surfactants, P85 and E₁₈P₁₈D₇₇E₁₈P₁₈, displaying better long-term stability. However, at a high ethanol level in solution, emulsions made with the shorter chained SPE surfactants E₇D₁₅E₇ and E₁₂D₁₅E₁₂ showed measurable stability, while those made with the other SPE surfactants were partially dispersible after shaking. On the contrary, the Pluronic surfactant P85 was not able to emulsify oil in water at all at a high ethanol level.

AFM measurement. AFM surface force curves were obtained in a liquid cell using Nanoscope IIIa (Digital Instruments). An E-scanner with a maximum scan area of 16 × 16 μm² was used. The *z* scale of the scanner was calibrated with the Ultra-Sharp Calibration Gratings TGZ02 set (step height 100 nm, Silicon-MDT). Silicon nitride (Si₃N₄) integral tips (NP type) were used with a manufacturer-specified spring constant of 0.22 N/m, a length of 120 μm, a width of 15 μm, and a nominal tip radius of 20 to 40 nm. The same cantilever was used in all the measurements discussed here unless specified in order to directly compare the force values. The spring constant of the cantilever was calibrated using the deflection method against a reference cantilever (Park Scientific Instruments) of known spring constant (0.157 N/m) (30). The measured spring constant 0.17 ± 0.05 N/m was used in the calculations of all the force curves. We did not determine the radius of curvature of the tip used in this study. However, methods exist to measure the AFM tip radius (31). The force calibration plot was converted to a force versus separation plot as described previously (5). Only approaching force curves are reported here. The tip to substrate velocity was fixed at 0.1 μm/s. We found that the force curves became independent of approach speed below 0.5 μm/s for the nonionic surfactant systems. The cantilever was irradiated by UV light from a fiber optical illuminator (Dolan-Jenner Industries) for more than 5 min before use, as suggested by the manu-

facturer. After the sample was brought to a close distance from the AFM tip, water was injected before the surfactant solution via silicone rubber tubing. Force curves were obtained in water to make sure that there was no contamination on the AFM tip. The surfactant solution was sealed within the cell by a silicone rubber O-ring and clamps. The force curves were obtained between 1 and 2 h after injection unless specified. The temperature was maintained at 22 ± 1°C.

RESULTS

The adsorption of the ABA triblock copolymeric surfactants was studied by directly measuring the surface force versus surface separation profiles between a hydrophobized silica substrate and an AFM tip in the water/ethanol solution at a fixed surfactant concentration. The purpose of this study was to understand the effect of molecular structure and solvent quality on the adsorption of the triblock surfactants. The adsorption behavior of silicone-based surfactants was compared to that of hydrocarbon-based Pluronic surfactants with a similar type of triblock structure.

General observation. AFM imaging of the substrate in the surfactant solution in the soft-contact mode (22, 32) yielded only flat, featureless images for both the SPE and Pluronic surfactants. Force profiles measured at different spots of the substrate in the surfactant solution were almost always identical to each other within the experimental uncertainty. It can therefore be concluded that the films formed by the triblock surfactants were uniform at the nanometer scale. In pure and mixed aqueous solutions of low ethanol level (<30%), all force curves shared a similar shape. At large separation, no force was detected. As the separation distance was gradually reduced, a repulsive force became measurable and it increased in magnitude. The repulsion reached a maximum value and was immediately followed by a discontinuity in the force measurement. At the end of discontinuity, the repulsion increased rapidly with further compression.

The first repulsion encountered during approach is attributed to the steric repulsion that originates from the force necessary to confine and desolvate the polyether chain of the adsorbed surfactants and to remove the surfactants from the tip and substrate contact zone. The onset of the steric repulsion corresponds to the unperturbed thickness of the surfactant film sandwiched between the tip and the substrate. In order to select the force onset uniformly, we arbitrarily chose the separation value at a force of 0.2 nN. This separation value is used here to describe the thickness of an “uncompressed” film, which we refer to as the steric barrier thickness. The discontinuity in the force measurement, often called the jump-in process, is caused by the mechanical instability of the cantilever spring. The jump-in corresponds to the removal of the adsorbed molecules between the tip and substrate, most probably by a lateral push-out mechanism. At the end of the jump-in, the spring is stabilized by the repulsion between the hard surfaces in contact. Previous study of polyoxyethylene surfactants suggests that most physically adsorbed

TABLE 5
Values of Steric Barrier Thickness and Height of Pluronic
Surfactants Measured in Pure Water

Pluronic surfactant	Barrier thickness (nm)	Barrier height (nN)
L62	—	—
L64	—	—
P65	13.5	2.9
F68	28.0	5.8
P84	11.9	1.6
P85	14.2	2.2
F87	14.8	3.7
F88	19.6	2.6
P104	15.1	5.7
P105	16.5	8.2
P108	24.5	7.4

Note. The symbol—indicates purely attractive force profile measured.

surfactant molecules are removed from the contact zone at the end of the jump-in process (32). Therefore, further deflection is attributed only to the bending of the cantilever spring. This assumption makes it possible to define the point of zero surface separation precisely and to equate the barrier thickness measured with the absolute value of the adsorbed film thickness. It is difficult to determine the adsorbed amount on the AFM tip. We attempted to shed some light on this vexing issue by using a hydrophilic substrate. The results will be discussed later in this paper. The value of the steric force maximum corresponds to the force necessary to remove the adsorbed film from the contact zone. It is an important parameter in colloidal and emulsion stabilization since the rate of colloidal coagulation is determined by the magnitude of the energy barrier. The steric barrier height was reported to be equal to the surface pressure of the surfactant film at the solid/liquid interface and proportional to the adsorbed amount (14). Therefore, we should be able to extract information about the packing density from the steric barrier height. The values of the steric barrier thickness and height of the Pluronic surfactants in water and of the SPE surfactants in the mixed solvent of water/ethanol are summarized in Table 5 and Fig. 1, respectively.

Silicone-based surfactants. The force-versus-separation curves for $E_7D_{15}E_7$ and $E_{12}D_{15}E_{12}$ in 0.2% w/w solution of mixed water/ethanol solvent are presented in Figs. 2 and 3, respectively. The two surfactants have identical B blocks of PDMS but different A blocks of PEO. $E_7D_{15}E_7$ formed a cloudy solution when the percentage of ethanol was below 22.6% v/v. The force data measured in a cloudy solution tend to have large scattering and therefore are not reported here. The surfactant with longer A blocks, $E_{12}D_{15}E_{12}$, formed clear solutions in all water/ethanol ratios. In Fig. 3, repulsion was detected between 15 and 4.1 nm, with a maximum of 8.6 nN in pure water for $E_{12}D_{15}E_{12}$. Its barrier thickness was determined to be 12.1 nm. As the level of ethanol was gradually increased, the magnitude

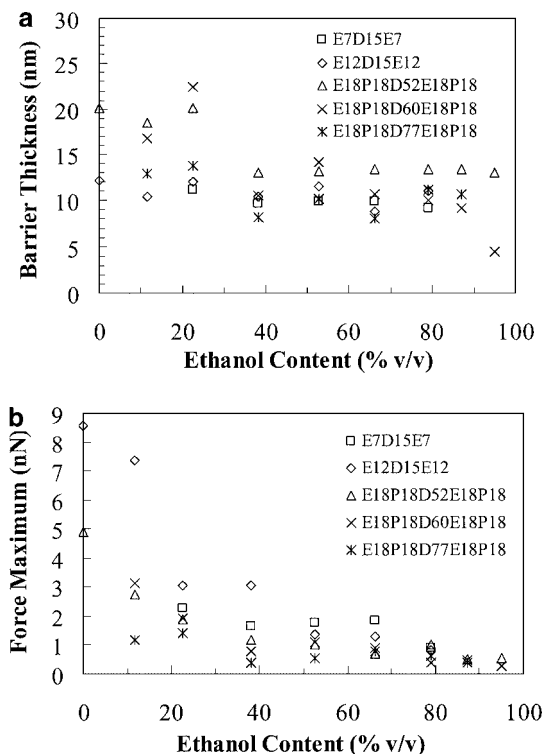


FIG. 1. Values of steric barrier thickness (a) and height (b) of ABA triblock SPE surfactants measured as a function of the ethanol content in solution.

of the steric barrier decreased. A similar trend was observed in the case of $E_7D_{15}E_7$, where both the steric barrier height and thickness were at their highest values, 2.3 nN and 11.1 nm, respectively, in 22.6% ethanol (the lowest ethanol level measured in this case due to the low solubility in water of the surfactant). At a high enough ethanol ratio (>80%), the net repulsion was replaced by a net attraction. At such high ethanol levels, these SPE surfactants are no longer surface active and provide no measurable steric barrier. In the case of $E_{12}D_{15}E_{12}$, the barrier height was drastically reduced during the initial addition of ethanol (Fig. 1b), while the barrier thickness remained almost

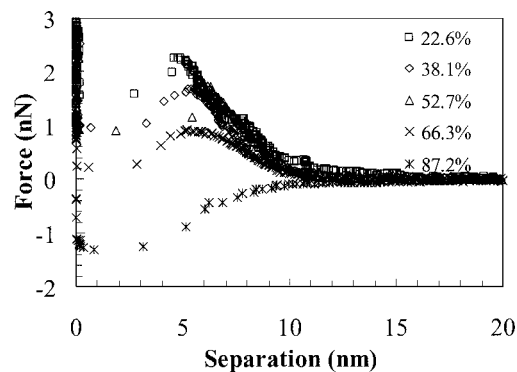


FIG. 2. Force versus distance profiles of 0.2% w/w $E_7D_{15}E_7$ in ethanol/water solutions with various volumetric ethanol contents.

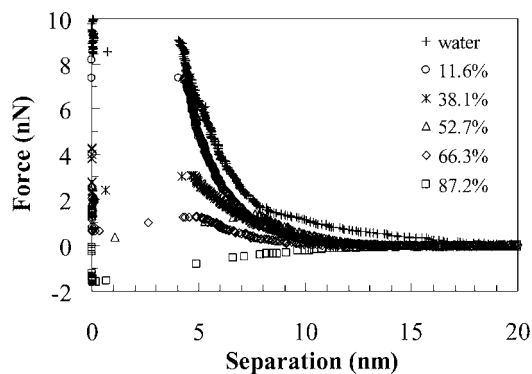


FIG. 3. Force versus distance profiles of 0.2% w/w $E_{12}D_{15}E_{12}$ in ethanol/water solutions with various volumetric ethanol contents.

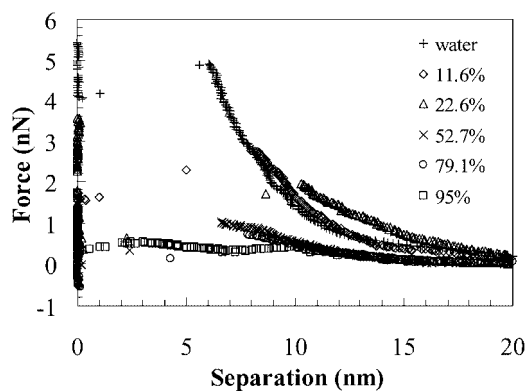


FIG. 4. Force versus distance profiles of 0.2% w/w $E_{18}P_{18}D_{52}E_{18}P_{18}$ in ethanol/water solutions with various ethanol contents.

constant at about 11 nm up to 80% ethanol (Fig. 1a). Similar behavior was found for the dodecyl polyoxyethylene surfactant $C_{12}E_{23}$ up to 30% ethanol (5). Such behavior suggests that the addition of ethanol reduces the amount of surfactant at the interface without significantly affecting the chain extension of the adsorbed surfactant. Organic solvents such as ethanol solubilize hydrocarbon moieties and therefore reduce the driving force for adsorption, while the film thickness, reflecting largely the extended hydrophilic polyoxyethylene configuration, remains unchanged in a good solvent, such as water and a mixed solvent of water and ethanol. In the case of $E_7D_{15}E_7$, we do not have data in pure water and at low ethanol levels to corroborate the initial trend, but above 22.6% v/v ethanol, both the thickness (~ 10 nm) and height (~ 2 nN) remained constant up to 80% ethanol. However, the data are incomplete because of the low solubility of $E_7D_{15}E_7$ in water.

The three higher molecular weight SPE triblock surfactants, $E_{18}P_{18}D_{52}E_{18}P_{18}$, $E_{18}P_{18}D_{60}E_{18}P_{18}$, and $E_{18}P_{18}D_{77}E_{18}P_{18}$, share identical an A block that contains randomly copolymerized PEO and PPO, but possess different B blocks. $E_{18}P_{18}D_{77}E_{18}P_{18}$ is end capped by acetoxy (OAc) instead of hydroxy (OH) groups. Previous force measurement of comb type SPEs indicated that surfactants with the same chain structure but different end capping groups displayed identical force curves (5). Therefore, we ignore the contribution of the end capping group here. $E_{18}P_{18}D_{52}E_{18}P_{18}$ at a 0.2% w/w concentration was clear in water and ethanol/water mixed solvents of all proportions. $E_{18}P_{18}D_{60}E_{18}P_{18}$ and $E_{18}P_{18}D_{77}E_{18}P_{18}$ formed only clear solution at ethanol contents $\geq 11.6\%$ v/v. Figure 4 shows the force versus distance profiles for $E_{18}P_{18}D_{52}E_{18}P_{18}$ in ethanol/water mixtures. In pure water, repulsion was detected between 20 and 5.6 nm, with a maximum of 4.9 nN. For all three higher molecular weight SPE surfactants both the barrier thickness and height decreased with increasing ethanol content (Fig. 1). One notable exception is the somewhat increasing barrier thickness between 11.6 and 22.6% v/v ethanol levels for all three surfactants. A similar phenomenon was also observed in comb SPE surfactants containing both PPO and PEO units and was attributed to

the unique solubility balance of PEO and PPO of the SPE surfactants (5). We found that the steric barrier in water and water-rich solvents decreased with increasing PDMS hydrophobe size.

Pluronic surfactants. In contrast to the SPE surfactants, the hydrocarbon-based surfactants and polymers lose their surfactancy in aqueous solutions above a certain threshold of alcohol level. In our previous study (5), the force curve measured in 0.2 mM $C_{12}E_{23}$ solution became purely attractive at about a 30% ethanol level. Figure 5 shows the surface force profiles in 0.5% w/w solutions of P85 ($EO_{26}PO_{39.5}EO_{26}$) with increasing ethanol content. In pure water, there existed a well-defined, monotonic repulsion that started at 13 nm and culminated at 5.5 nm, with a maximum of 4.7 nN. The force maximum is less than that of $C_{12}E_{23}$ and $E_{12}D_{15}E_{12}$ but closer in value to that of $E_{18}P_{18}D_{60}E_{18}P_{18}$. It is possible that the packing density is reduced by either the bulkier hydrophiles and/or the bulkier hydrophobes. The film thickness is larger than the hydrodynamic thickness based on measurement by photon correlation spectroscopy on a styrene latex surface (6.0 nm) (9) or even the fully extended chain length (9.6 nm). Several possible factors may account for the longer than expected film thickness. First,

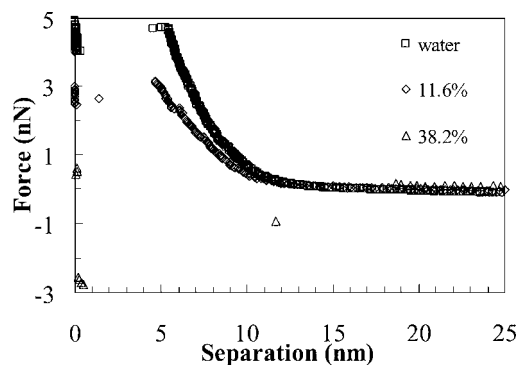


FIG. 5. Force versus distance profiles of 0.5% w/w P85 in ethanol/water solutions with various volumetric ethanol contents.

P85 may form micellar aggregates on OTS because it has been reported that the adsorbed film of P85 is in equilibrium with unimers (1.8 nm in hydrodynamic radius), micelles (8 nm in hydrodynamic radius), and micellar aggregates (size greater than 80 nm) (33). But this is unlikely since no aggregate structure was detected in AFM images captured in the soft-contact mode. In addition, the force curves should show multiple jump-in points for more than one layer of micelles. A second possible factor is the polydispersity of the sample that tends to lengthen the tail portion of the force curve. A third possibility is that P85 forms a micelle- or bilayer-like structure on the hydrophilic AFM tip. We discuss this possibility later in the paper in conjunction with the description of the force curves measured between hydrophilic surfaces. Despite the inherent uncertainty associated with film thickness determination by AFM, the most probable structure for P85 on OTS is a monolayer structure. The force maximum decreased to 3.0 nN in 11.6% v/v ethanol and disappeared completely at 38.2% v/v ethanol. The attraction at 38.2% v/v is longer than that resulting from pure VDW attraction (<3 nm), suggesting possible bridging forces by sparsely adsorbed surfactant molecules. Except for L62 and L64, which offered no steric repulsion even in pure water, all the other Pluronic surfactants we studied behaved in a manner similar to P85 in that the steric repulsion diminished when the ethanol level rose above 40%. This agrees well with a well-known fact of conventional hydrocarbon surfactants, that is, they lose their surface activity and the ability to form micelles in the presence of 25% or more ethanol (19). The AFM force curves also agree qualitatively with our emulsion stability study. In formulations that require more than a 30% ethanol level, only SPE surfactants will be able to maintain their surfactancy.

In water, the force profiles of the Pluronic surfactants were found to vary with both PEO and PPO chain length, as shown in Table 5. The general trend points to an increase in the steric force barrier, both in thickness and height, with increasing PEO chain length when the PPO chain length is fixed. However, in the case of surfactants with similar PEO chain lengths, no clear correlation seems to exist between the steric force barrier and the hydrophobic PPO chain length.

Adsorption on hydrophilic surfaces. In order to estimate the amount of surfactant adsorption on the AFM tip, force versus separation curves were obtained between the AFM tip and a bare oxidized silicon wafer in the same surfactant solutions. Oxidized silicon nitride contains acidic SiOH and basic SiNH₂ groups and is considered hydrophilic. Force curves in 0.2% w/w E₇D₁₅E₇ and E₁₂D₁₅E₁₂ were obtained in mixed solvents containing from 11.6 to 66.3% v/v of ethanol. In the absence of a clear jump-in process, the point of zero separation was determined by selecting the region of high and constant compliance. Repulsion was observed at a separation of 2 nm and increased steeply with distance, significantly shorter ranged than those measured on the hydrophobized silica surface. Similar results were observed for other ABA triblock and comb type SPE surfactants. It shows that the ethoxylated surfactants form a thin

yet strongly bound film on silica. Other studies of the Pluronic surfactants also found that the adsorbed film was rather thin, 2 to 5 nm in hydrodynamic thickness, on hydrophilic silica (34, 35). We may conclude that there exists a nonnegligible but minor contribution from the surfactant adsorbed at the AFM tip to the overall steric force profile measured here. We arrived at this conclusion based on several factors. First the very short-range interaction between two hydrophilic substrates, i.e., oxidized silicon and silicon nitride, means that the long-range repulsion encountered in cases where the oxidized silicon substrate is covered by an OTS monolayer up to the jump-in point is largely employed to remove the surfactant adsorbed at the hydrophobic solid/solvent interface. Second, after the jump-in process, the remaining film at the AFM tip was treated as part of the hard surface in our conversion from the deflection versus distance curve to the force versus separation curve, since the rising of repulsion due to the remaining thin layer on the tip is so steep that it is almost indistinguishable from a hard contact repulsion. This effectively eliminates the overestimation of the film thickness at the hydrophobic surface. Therefore, the extracted barrier thickness should closely resemble the surfactant layer thickness on the OTS-covered substrate.

Adsorption kinetics. The adsorption kinetics of triblock SPEs on OTS monolayers was studied. The force curves in an SPE solution sealed in a liquid cell were recorded as a function of time. Figure 6 shows the surface force curves for 0.2% w/w E₁₈P₁₈E₅₂E₁₈P₁₈ in pure water on an OTS surface obtained at time intervals ranging from 10 min to 15 h after injection. The data showed little change with time beyond 1 h. The same behavior was also observed in a mixed solvent of water/ethanol and for E₁₈P₁₈E₆₀E₁₈P₁₈ and E₁₈P₁₈E₇₇E₁₈P₁₈. We concluded that the adsorption of triblock SPE surfactants was fast and the system reached equilibrium within 1 h. We also did not observe any hysteresis in force curves measured during consecutive compressions. Despite the polymeric nature of the SPE surfactants, the flexible siloxane chain seems to aid fast adsorption and packing of the surfactants at the solid/liquid interface. In fact, Fig. 6 displays typical experimental uncertainties in our AFM force

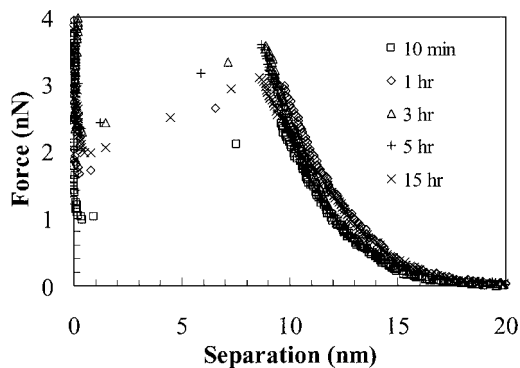


FIG. 6. Force versus distance profiles of 0.2% w/w E₁₈P₁₈D₅₂E₁₈P₁₈ in water measured at different time intervals after the initial injection of the solution.

measurement, with an estimated error bar of ± 0.16 nN for the force magnitude and an error of ± 0.5 nm for the separation distance.

DISCUSSION

Relationship between the steric force profile and hydrophilic/hydrophobic block size. At low Pluronic surfactant concentrations (well below CMC), while the PPO segments adhere to the hydrophobic surface, the PEO segments may also adhere to the hydrophobic surface in a flat configuration. However, at the point of pseudo surface saturation, as in the case here, the adsorption configuration for triblock surfactants on hydrophobic surfaces is the buoy–anchor–buoy configuration. We measured the surface force profiles of BAB type triblock surfactants PPO-PEO-PPO (Pluronic R Series, BASF) on an OTS surface in water using the same AFM technique and found only purely attractive profiles (36). Apparently, the anchor–buoy–anchor does not provide nearly as much steric forces as the buoy–anchor–buoy configuration.

In the buoy–anchor–buoy configuration, the barrier thickness is expected to increase with the hydrophilic block size. Figure 7a plots the measured steric barrier thickness against the number of EO units for all the Pluronic surfactants studied here.³ It shows that in the case of Pluronic surfactants, the barrier thickness increases steadily with the A block size. The two SPE surfactants E₇D₁₅E₇ and E₁₂D₁₅E₁₂ display longer than expected thickness when compared with the Pluronic surfactants. In the same figure, the AFM results are compared with calculations based on fully extended chain, helical chain, and random coil configurations of polyoxyethylene.⁴ All the AFM data points lie in the vicinity of the calculated length of the fully extended chain. As mentioned earlier, the AFM-measured film thickness may disproportionately reflect the contributions from longer chains in the highly polydispersed samples. A more meaningful way to analyze the barrier thickness data is to extract a characteristic exponential decay length from the central portion of the steric force profile, since the steric repulsion between the polymer brushes is roughly an exponential function of separation (39). We plotted the logarithmic decay length, obtained from the slope of the semilogarithmic plot of force versus separation, against the logarithmic number of EO units in Fig. 7b. It shows a fairly linear line, with the exception of a couple of data points at the low EO number end with the least squares fit slope of 0.62. Others also measured 0.6 scaling constant on end-adsorbed chains in a good solvent (40). This scaling law comes from the constant free energy per chain for physically adsorbed chains and the in-

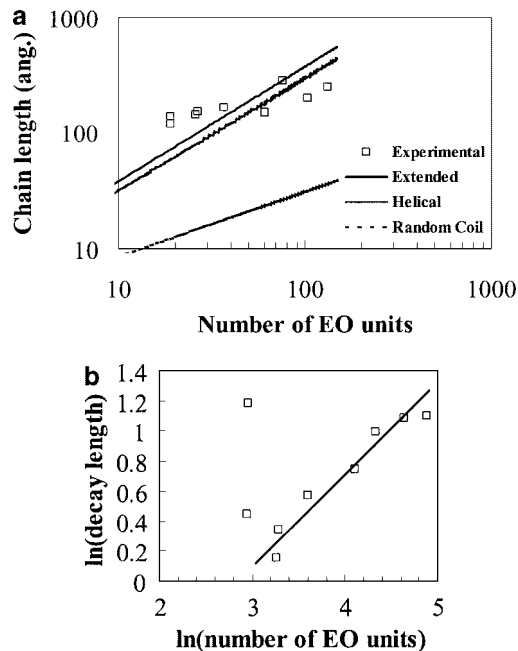


FIG. 7. (a) Plot of the steric barrier thickness measured in aqueous solutions of Pluronic surfactants versus the number of EO units in the A block. The straight lines are calculations of the A block chain length versus the number of EO units based on fully extended, helical, and random coil configurations. (b) Plot of the steric force decay length versus the number of EO units (open squares). The straight line is drawn to guide the eye.

teranchor spacing that scales with the swollen coil-like size of the hydrophilic block in a good solvent. The hydrophilic blocks are less stretched than true polymer brushes. Again, the decay lengths of the SPE surfactants are significantly higher than those from the scaling fit.

While the film thickness is largely determined by the size of the hydrophilic block, the hydrophobic block seems also to affect the overall steric barrier thickness. The majority of data from low to intermediate ethanol levels show that the barrier thickness increases with decreasing PDMS chain length for SPE surfactants with a fixed hydrophilic chain length. The observed increase in both the barrier thickness and height with decreasing B block size is consistent with the “pancake” model, in which the anchor block covers an amount of surface corresponding to the projected area of the poorly solvated anchor block (41). A more compact anchor block lowers the interchain spacing among the buoy blocks and causes them to stretch more. Pluronic surfactants were shown to exhibit an opposite trend, i.e., an increase in the steric barrier thickness and height with increasing PPO chain length, in the literature (9). This was attributed to an increased affinity of a larger PPO block to the hydrophobic substrate. However, our AFM force measurement data did not yield any clear trend between the PPO block size and steric barrier for the Pluronic surfactants.

Relationship between the steric force profile and surfactant molecular architecture. Assuming that the steric barrier height

³ The data were taken from the force profiles measured either in pure water or in a clear solution with a minimum ethanol percentage when the surfactant solution in pure water was cloudy.

⁴ Fully extended chain length = $3.7 \times N$ (Å). Helical chain length = $0.967 \times (3N + 2)$ (Å). Radius of random coil = $2.40 \times N^{0.55}$ (Å). N is the number of EO units. The helical chain length calculation is based on a formula in a paper by Craven *et al.* (37). The random coil length calculation is based on a formula in a paper by Bhat and Timasheff (38).

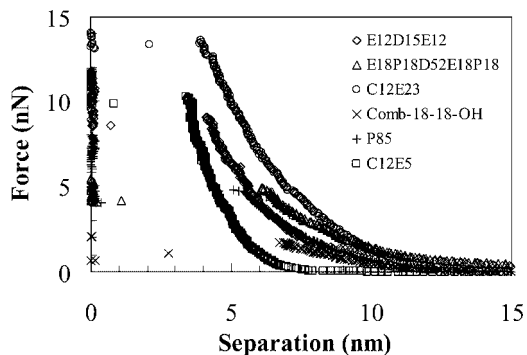


FIG. 8. Force versus distance profiles of 0.2 mM $C_{12}E_5$, 0.2 mM $C_{12}E_{23}$ (taken from Reference 6 with permission), 0.5% w/w P85 ($E_{26.0}P_{39.5}E_{26.0}$), 0.2% w/w $E_{12}D_{15}E_{12}$, 0.2% w/w $E_{18}P_{18}D_{52}E_{18}P_{18}$, and 0.2% w/w comb-18-18-OH (taken from Reference 6 with permission. The surfactant has the structure $MD_{108}D'_{10}M$, where $M = (CH_3)_3SiO_{1/2}$, $D = (CH_3)_2SiO_{1/2}$, $D' = (CH_3)RSiO_{1/2}$, and $R = (CH_2)_3-(EO)_{18}-(PO)_{18}-OH$) between an AFM tip and an OTS monolayer in aqueous solution. The force curves of $E_{18}P_{18}D_{52}E_{18}P_{18}$ and comb-18-18-OH were obtained with different AFM tips; the rest were obtained using the same AFM tip.

is proportional to the force necessary to remove the surfactant film from the substrate surface, we attempted to learn the influence of the surfactant architecture on surfactant ability to provide steric stabilization against colloidal coagulation. We compared a series of surfactants from our current and a previous study with different chain architecture and compositions by plotting their force curves together in Fig. 8. All the surfactants display finite steric barriers, indicating that all are capable of providing a certain degree of colloidal stability in water. The steric barrier height varies with the surfactant architecture. Low-molecular-weight, single-chained surfactants, such as $C_{12}E_{23}$ and $C_{12}E_5$, display the strongest repulsion, suggesting that a linear structure allows the closest chain packing. The next group, triblock Pluronic and SPE surfactants, gives an intermediate level of repulsion. Within the same group, the ones with smaller molecular weight, such as $E_{12}D_{15}E_{12}$, provide stronger repulsion than the higher molecular weight type, such as $E_{18}P_{18}D_{52}E_{18}P_{18}$ and $E_{26.0}P_{39.5}E_{26.0}$ (P85). The surface tension measurement at the air/solution interface showed that the area per molecule was smaller for the lower molecular weight surfactants at CMC (Table 3). The closer packing of the smaller molecules may account for their stronger repulsion at the solid/liquid interface. The comb type SPE surfactants offer the least steric force against colloidal coagulation. The long anchoring backbone of a comb polymer prevents close packing of the buoy polyether chains. These force measurement results are consistent with known arts in common emulsion formulation practice. It is fair to say that conventional, short-chained surfactants, such as the ethoxylated fatty alcohols, are found to be more effective emulsifiers in general than polymeric surfactants, such as Pluronics and SPEs, regardless of the oil phase being hydrocarbon or silicone. Short-chained surfactants diffuse faster to the interface than their longer chained counterparts. Of course, exceptions exist, for example, in the

case when the PPO or siloxane segments of a SPE surfactant are very soluble in or compatible with a low-molecular-weight oil phase, the surfactant becomes a very efficient emulsifier. The polymeric surfactants can, however, provide certain unique stabilization properties as cosurfactants that their conventional short-chained counterparts lack. The alcohol-stable emulsions are one such example that is clearly demonstrated in here.

Relationship between the surfactant adsorption in alcoholic media and surfactant molecular structure. AFM force measurements show that the steric barrier no longer exists when the ethanol level is above 40% for hydrocarbon-based surfactants and polymers. On the other hand, the SPE surfactants are capable of providing steric stabilization at a hydrophobic surface up to the 80% ethanol level in the case of $E_7D_{15}E_{17}$ and $E_{12}D_{15}E_{12}$ and up to 95% ethanol in the case of $E_{18}P_{18}D_kE_{18}P_{18}$ ($k = 52, 60,$ and 77) and comb type SPE surfactants. The force measurement results are consistent with the findings from emulsion stability studies. At intermediate to high alcohol levels, hydrocarbon-based surfactants such as $C_{12}E_{23}$ and Pluronics do not emulsify oil in water, while all the SPE surfactants studied maintain some degree of emulsifying capability. Our force measurement also found that the triblock SPE surfactants with the copolymers of PEO and PPO withstand higher alcohol levels than those with PEO homopolymers as the polyether chain. The same conclusion was supported by our previous study on comb SPE surfactants (5). In addition, both studies found that the steric barrier of the SPE surfactants with PPO units showed a maximum in either the barrier thickness or the barrier height when ethanol was at an intermediate level, usually somewhere between 20 and 40%. However, the film thickness dependence on the balance between chain desorption and chain unwinding in the presence of ethanol may be different from that of the steric barrier height. Knowledge of the adsorbed amount, i.e., adsorption isotherms, is needed in order to understand this delicate balance quantitatively. Emulsions made with comb SPE surfactants with balanced EO and PO units also showed stability up to the 80% ethanol level. This phenomenon is attributed to the oleophobicity of siloxane chains with molecular weights above 1000 as well as an appropriate solubility balance of PEO and PPO in alcoholic media. The polysiloxane chain anchors the surfactant at the adsorbent surface in alcoholic media, and the steric barrier is finely tuned by the water-insoluble PO to water-soluble EO ratio in the polyether chain. The most advantageous applications of the SPE surfactants are in the emulsification and stabilization of silicone oil-in-water emulsions as cosurfactants where the water phase contains a significant level of alcohol cosolvents (17). In order to maintain constant surfactancy in formulations with varying ethanol levels, the surfactant should have one type of segment with balanced EO and PO units and other segments that are both hydrophobic and oleophobic. The same mechanism responsible for colloidal and emulsion stabilization in alcoholic media may also apply to formulations involving other organic solvents.

SUMMARY

The steric interaction provided by the ABA triblock silicone polyether and polyoxyethylene-polyoxypropylene-polyoxyethylene Pluronic surfactants adsorbed at the interface of an *n*-octadecyltrichlorosilane monolayer and surfactant solution in alcoholic media were measured using atomic force microscopy. It was found that steric repulsion persisted to the 80% ethanol level in silicone surfactant solutions but only to 40% in Pluronic surfactant solutions. The force measurement results are consistent with the findings of emulsion stability measurements. These silicone surfactants are appropriate cosurfactants in emulsion and dispersion products and processes that involve alcohols or other organic solvents. In addition, the steric force profiles can be tuned or kept unchanged in a wide range of alcohol levels by the ratio of oxyethylene to oxypropylene units in the polyether chain of the silicone surfactants.

According to our results in aqueous solutions, single-chained surfactants offer the highest steric repulsion, followed by triblock surfactants. The high-molecular-weight comb surfactants offer the weakest steric repulsion. It is concluded that surfactants that possess architecture for close packing at the interface are likely to offer the highest resistance against colloidal coagulation. The steric force barrier increases with increasing hydrophilic block size in aqueous solutions of triblock silicone and Pluronic surfactants. The characteristic force decay length of Pluronic surfactants is proportional to (number of oxyethylene units)^{0.62}, reflecting the swollen coil-like configuration of a hydrophilic block anchored by a hydrophobic block in a good solvent. Silicone surfactants showed significantly higher film thickness than Pluronic surfactants with similar hydrophilic block sizes. The greater than expected film thickness may be caused by the polydispersity of the samples. The adsorption of the surfactants on the AFM tip is concluded to alter little the estimated steric force barrier thickness and height of the surfactant film adsorbed on the hydrophobic surface. The steric force barrier increases with decreasing polysiloxane chain length and is attributed to the "pancake" configuration in which the anchor block covers an amount of surface corresponding to the projected area of the poorly solvated anchor block.

ACKNOWLEDGMENTS

We acknowledge Jinping Dong for conducting the surface tension measurement. Professor G. Mao acknowledges financial support from the National Science Foundation (CTS-9703102) and the Petroleum Research Fund (36149-AC5).

REFERENCES

- Napper, D. H., "Polymeric Stabilization of Colloidal Dispersions." Academic Press, London, 1983.
- Halperin, A., Tirrell, M., and Lodge, T. P., *Adv. Polym. Sci.* **100**, 31 (1992).
- Milner, S. T., *Science* **21**, 905 (1991).
- Hill, R. M., in "Silicone Surfactants" (R. M. Hill, Ed.), Chap. 1. Dekker, New York, 1999.
- Wang, A., Jiang, L., Mao, G., and Liu, Y., *J. Colloid Interface Sci.* **242**, 337 (2001).
- Alexandridis, P., and Hatton, T. A., *Colloids Surf. A* **96**, 1, 1995.
- Almgren, M., Brown, W., and Hvidt, S., *Colloid Polym. Sci.* **273**, 2 (1995).
- Mortensen, K., and Brown, W., *Macromolecules* **26**, 4128 (1993).
- Shar, J. A., Obey, T. M., and Cosgrove, T., *Colloids Surf. A* **136**, 21 (1998).
- Li, J.-T., Caldwell, K. D., and Rapoport, N., *Langmuir* **10**, 4475 (1994).
- Baker, J. A., and Berg, J. C., *Langmuir* **4**, 1055 (1998).
- Yang, J., and Wegner, G., *Macromolecules* **25**, 1786 (1992).
- Hill, R. M., He, M., Lin, Z., Davis, H. T., and Scriven, L. E., *Langmuir* **9**, 2789 (1993).
- Eskilsson, K., Ninham, B. W., Tiberg, F., and Yaminsky, V. V., *Langmuir* **15**, 3242 (1999).
- Eskilsson, K., Grant, L. M., Hansson, P., and Tiberg, F., *Langmuir* **15**, 5150 (1999).
- Karin, S., Claesson, P. M., Malmsten, M., Linse, P., and Booth, C., *J. Phys. Chem. B* **101**, 4238 (1997).
- Vincent, J., and Gee, R., U.S. patent 5891954.
- Vincent, J., Liu, Y., and Liles, D., U.S. patent pending.
- Zana, R., *Adv. Colloid Interface Sci.* **57**, 1 (1995).
- Ducker, W. A., Senden, T. J., and Pashley, R. M., *Nature* **353**, 239 (1991).
- Israelachvili, J. N., and Adams, G. E., *J. Chem. Soc., Faraday Trans. 1* **74**, 975 (1978).
- Patrick, H. N., Warr, G. G., Manne, S., and Aksay, I. A., *Langmuir* **13**, 4349 (1997).
- Grant, L. M., Ederth, T., and Tiberg, F., *Langmuir* **16**, 2285 (2000).
- LeGrow, G. E., and Petroff, L. J., in "Silicone Surfactants" (R. M. Hill, Ed.), Chap. 2. Dekker, New York, 1999.
- Adams, A. W., and Gast, A. P., "Physical Chemistry of Surfaces," 6th ed. Wiley, New York, 1997.
- Beerbower, A., and Hill, M. W., "McCutcheon's Detergents and Emulsifiers," pp. 223-235. Allured, Ridgewood, New Jersey, 1971.
- Beerbower, A., and Hill, M. W., *Am. Cosmetics Perfumery* **87**, 85 (1972).
- Kern, W., *J. Electrochem. Soc.* **137**, 1887 (1990).
- Wu, B., Mao, G., and Ng, K. Y. S., *Colloids Surfaces A* **162**, 203 (1999).
- Tortonese, M., and Kirk, M., *SPIE* **3009**, 53 (1997).
- Shieko, S. S., Moller, M., Reuvekamp, E. M. C. M., and Zendbergen, H. W., *Phys. Rev. B* **48**, 5675 (1993).
- Dong, J., and Mao, G., *Langmuir* **16**, 6641 (2000).
- Brown, W., Schillen, K., Almgren, M., Hvidt, S., and Bahadur, P., *J. Phys. Chem.* **95**, 1850 (1991).
- Tiberg, F., Malmsten, M., Linse, P., and Lindman, B., *Langmuir* **7**, 2723 (1991).
- Malmsten, M., Linse, P., and Cosgrove, T., *Macromolecules* **25**, 2474 (1992).
- Wang, A., and Mao, G., unpublished results.
- Craven, J. R., Hao, Z., and Booth, C. J., *Chem. Soc. Faraday Trans.* **87**, 1183 (1991).
- Bhat, R., and Timasheff, S. N., *Protein Sci.* **1**, 1133 (1992).
- Israelachvili, J., "Intermolecular and Surface Forces," 2nd ed., p. 295. Academic Press, London, 1992.
- Taunton, H. J., Toprakcioglu, C., Fetters, L. J., and Klein, J., *Macromolecules* **23**, 571 (1990).
- Hadziioannou, G., Patel, S., Granick, S., and Tirrell, M., *J. Am. Chem. Soc.* **108**, 2869 (1986).